

The DDX39B/FUT3/TGF β R-I Axis Promotes Tumor Metastasis and EMT in Colorectal Cancer

Chengcheng He

Southern Medical University Nanfang Hospital

Aimin Li

Southern Medical University Nanfang Hospital

Qihua Lai

Southern Medical University Nanfang Hospital

Jian Ding

Southern Medical University Nanfang Hospital

Qun Yan

Southern Medical University Nanfang Hospital

Side Liu

Southern Medical University Nanfang Hospital

Qingyuan Li (✉ liqingyuan09@smu.edu.cn)

Southern Medical University Nanfang Hospital

Research

Keywords: DDX39B, Colorectal cancer, Metastasis, Alternative splicing, mRNA export, Fucosylation.

Posted Date: July 17th, 2020

DOI: <https://doi.org/10.21203/rs.3.rs-42529/v1>

License:  This work is licensed under a Creative Commons Attribution 4.0 International License. [Read Full License](#)

Abstract

Background: DDX39B is a member of the DEAD box (DDX) RNA helicase family required for nearly all cellular RNA metabolism processes. The exact role and potential molecular mechanism of DDX39B in the progression of human colorectal cancer (CRC) remain to be investigated.

Methods: Western blotting and quantitative real-time PCR (qRT-PCR) were conducted to detect the expression of DDX39B in CRC tissues and cell lines. Transwell and wound healing assays were conducted to assess the migration and invasion ability of CRC cells with DDX39B overexpressed or silencing. Orthotopic transplantation model of nude mice was performed to validate CRC metastasis in vivo. RNA sequencing (RNA-seq) and RNA binding protein immunoprecipitation (RIP) assay verified the direct regulation of DDX39B on the splicing and nuclear export of FUT3 mRNA, cytoplasmic and nuclear RNA isolation confirmed the nuclear export effect of DDX39B on FUT3. qRT-PCR was conducted to quantify FUT3 splicing variants. Lectin blotting was conducted to evaluate the fucosylation level of TGF β R-I.

Results: In the present study, we demonstrate that DDX39B expression was higher in CRC tissues than in adjacent normal tissues. Gain- and loss- of- function assays revealed that DDX39B facilitated the metastasis of CRC in vivo and in vitro. Mechanistically, RNA-seq and RIP showed that DDX39B upregulated FUT3 expression by binding the first exon of FUT3 mRNA, which promote the mRNA splicing and export of FUT3. RNA-seq results and qRT-PCR showed that overexpression of DDX39B may favor the longer FUT3 mRNA products that contain the complete and longer exon 2, suggesting an alternative splicing of FUT3. Upregulation of FUT3 accelerated the fucosylation of TGF β R-I, thus activating the TGF β /SMAD signaling pathway, eventually driving the epithelial-mesenchymal transition (EMT) program and contributing to CRC progression.

Conclusions: Our finding demonstrated for the first time that the DDX39B/FUT3/TGF β R-I axis promotes the progression of CRC. These findings not only provide new insight into the role of DDX39B in mRNA splicing and export and tumorigenesis, but also shed light on the effect of aberrant fucosylation on CRC progression.

Background

Colorectal cancer (CRC) is among the most common malignant cancers worldwide, and the high mortality rate of CRC has made it a major health burden. [1] Though a certain degree of progress has been made in the diagnosis and treatment of CRC, the overall prognosis of patients with CRC remains low, as tumor relapse and metastasis pose a great challenge to both clinicians and patients. Thus, considerable research on the molecular understanding of CRC metastasis is urgently need. The TGF β signaling pathway plays a crucial role in cancer metastasis via angiogenesis, the epithelial-mesenchymal transition (EMT) program and extracellular matrix (ECM) degradation. [2-4] Therefore, the TGF β signaling pathway may render certain genes capable of promoting cancer metastasis. [5-7]

Members of the DEAD box (DDX) RNA helicase family are characterized by the presence of a conserved amino sequence (Asp-Glu-Ala-Asp) and required for virtually all cellular RNA metabolism processes, including transcription, splicing, ribosome biogenesis, nuclear export, translation and degradation. [8, 9] Hence, deregulation of DDXs may result in the disruption of RNA processing and exert detrimental effects on the expression of certain key genes, such as oncogenes and tumor suppressors. [10-12] Therefore, cancer cells may rely on DDXs to attain increased expression of oncogenes and decreased production of tumor suppressors to promote cancer survival.

DDX39B is a well-studied RNA helicase in terms of its enzymatic activity and properties in RNA metabolism. [13, 14] Notably, DDX39B is a pivotal splicing factor that promotes recruitment of the spliceosome and RNA export adaptor complexes, such as the exon-junction complex (EJC) and transcription-export complex (TREX). [15-17] These complexes are recruited to mRNA in the nucleus and assist the cytoplasmic localization of RNA. However, the function of DDX39B in diseases such as cancer is largely unexplored and remains to be studied. DDX39A, a paralog of DDX39B, has been shown to have cancer-promoting activity in lung squamous-cell carcinoma, urinary bladder cancer, human malignant pleural mesothelioma and hepatocellular carcinoma. [18-22] These findings prompted us to investigate whether DDX39B has oncogenic or tumor suppressive potential in the progression of CRC.

In the current study, we explored the exact role and molecular interactions of DDX39B in the development of CRC. Herein, we report that DDX39B promoted CRC metastasis in vitro and in vivo. Moreover, we found that DDX39B might modulate FUT3 expression by regulating the mRNA splicing and nuclear export of FUT3, resulting in the aberrant fucosylation of TGF β R-I, thus influencing activation of the TGF β signaling pathway. Taken together, our results demonstrate a mechanism for the involvement of the DDX39B/FUT3/TGF β R-I axis in the progression of CRC.

Materials And Methods

Clinical specimens

Human CRC tissues and adjacent normal colon tissues in our study were obtained from CRC patients who underwent surgical resection at Nanfang Hospital of Southern Medical University. A diagnosis of CRC was confirmed histopathologically for each sample. The protocols used in this study were approved by NanFang Hospital's Protection of Human Subjects Committee.

Immunohistochemical (IHC) and Hematoxylin and eosin (HE) staining

See supplementary materials and methods for details.

Cell culture

Human CRC cell lines (SW480, SW620, HT29, HCT116, RKO, LoVo) were purchased from the Cell Bank of Type Culture Collection (CBTCC, China Academy of Sciences, Shanghai, China). All cells were cultured in Dulbecco's modified Eagle's medium (DMEM) (Gibco, Carlsbad, CA) supplemented with 10% fetal bovine serum (FBS; Gibco, Carlsbad, CA) at 37°C with a humidity of 5% CO₂.

Small interfering RNA and lentivirus transfection

See supplementary materials and methods for details.

Western blotting and lectin blotting analyses

See supplementary materials and methods for details.

Total, cytoplasmic and nuclear RNA isolation and quantitative real-time PCR (qRT-PCR)

See supplementary materials and methods for details.

Migration and invasion assays

See supplementary materials and methods for details.

Immunofluorescence

See supplementary materials and methods for details.

RNA-sequencing (RNA-seq)

We sent SW480/Vector and SW480/DDX39B cells to BGI China. Total RNA was extracted using TRIzol reagent (Invitrogen, Carlsbad, CA, USA). After the total RNA was qualified and quantified, oligo(dT)-attached magnetic beads were used to purify the mRNA. Following by mRNA fragmentation, reverse transcription and amplification, the single strand circle DNA was formatted for the final library construction. DNA nanoballs were loaded into the patterned nanoarray and single end 50 base reads were generated on the BGISEQ500 platform (BGI-Shenzhen, China). RNA-seq results were visualized with the Broad Institute's Integrative Genomic Viewer.

RNA-binding protein immunoprecipitation(RIP)

Magna RIP Kit (Billerica MA, USA, No.17-701) was used for RIP. 2×10⁷ of SW480/DDX39B cells (per immunoprecipitation) were collected first, according to the detailed specification of Magna RIP Kit. 10μl of antibody against the DYKDDDDK Tag (#66008-3, Proteintech) were used for RIP.

Tumorigenesis in nude mice

To generate the orthotopic transplantation model, SW480/Scramble and SW480/shDDX39B cells (1×10⁷) were injected into the ileocecal serosa of 4-6week old male BALB/c athymic mouse (nu/nu). All mice were purchased from the Medical Animal Center of Guangdong Province (Guangzhou, China), and housed under specific pathogen-free conditions, and the animal protocols were approved by the Use Committee for Animal Care. After 8 weeks, the mice were killed and their tumors were then paraffin-embedded. HE staining was performed to detect metastasis of the spleen, and the orthotopic tumors were subjected to IHC staining and immunofluorescence assay.

Statistical analyses

Statistical analyses were performed using SPSS 22.0 (IBM; Chicago, IL, USA) and Microsoft Excel 2016 (Microsoft, Redmond, WA, USA). Student's t test was applied for comparisons between groups. Correlation analysis was assessed by determining the Spearman's rank correlation coefficient (*P<0.05, **P<0.01, ***P<0.001 indicated significance.).

Results

DDX39B was dysregulated in CRC tissues and cells

Analysis of data from The Cancer Genome Atlas (TCGA) database^[23] suggested that DDX39B (also called BAT1) was overexpressed in CRC samples compared with normal samples, and that the expression of DDX39B was higher in cancers of different histological types and stages to varying degrees (Fig. 1A). Moreover, Kaplan-Meier survival analysis of overall survival in CRC patients revealed that patients with high DDX39B expression levels had a shorter overall survival time than patients with low DDX39B expression levels (Fig. 1B). A similar result was obtained from data in the PROGgeneV2-Pan Cancer Prognostic Database (Fig. 1C).

To evaluate DDX39B expression levels in CRC, we conducted western blotting, qRT-PCR assays and IHC. 12 pairs of human CRC tissues were detected by western blotting, which exhibited the up-regulation of DDX39B in CRC tissues compared to adjacent normal tissues (Fig. 1F). The detection of DDX39B in 74 paired CRC tissues by qPCR assay confirmed this finding (Fig. 1D). By means of IHC, we also found the increased expression of DDX39B in CRC tissues compared to matched normal tissues (Fig. 1E). Furthermore, we detected the expression level of DDX39B in six CRC cell lines by western blotting. DDX39B expression was highest in RKO cells, low in HT29, HCT116, SW620, LoVo cells, and moderate in SW480 cells (Fig. S1A).

DDX39B enhanced the migration and invasion abilities of CRC cells in vitro and in vivo

To explore the biological function of DDX39B in CRC, we first examined the transfection efficiency in CRC cells with DDX39B overexpressed and knockdown using western blotting, qRT-PCR (Fig. 2A-B) and immunofluorescence (Fig. S1B). To detect the migration and invasion properties of CRC cells with DDX39B overexpression or silencing, Transwell and wound healing assays were conducted. As shown in Figure 2C-D and Figure S1C-E, the number of migrated and invaded cells were higher in HCT116/DDX39B and SW480/DDX39B cells than in HCT116/Vector and SW480/Vector cells. Upon the depletion of DDX39B, we observed a significant decrease in cell migration and invasion in the RKO/siDDX39B_1, RKO/siDDX39B_2, SW480/siDDX39B-1 and SW480/siDDX39B_2 groups. Taken together, DDX39B enhanced the migration and invasion capacities of CRC cells.

To validate our findings in vivo, an orthotopic transplantation model of CRC was established in the mice. Notably, more spleen metastases were observed in the SW480/Scramble group than in the SW480/shDDX39B group (Fig. 3A).

DDX39B facilitates the EMT program in CRC

Because the EMT program is a key process that contributes to CRC metastasis,^[24] we detected the role of EMT in CRC cells with DDX39B overexpression and silencing. As the EMT program may be impaired in microsatellite unstable cells, such as the HCT116 cell line^[25], we conducted the EMT assay in SW480 cells. Western blotting assay showed that the increased expression levels of Vimentin, MMP2/3/9, SNAIL, SLUG and ZEB1 and decreased expression level of E-cadherin in SW480/DDX39B group than in SW480/Vector group. In contrast, the opposite effect was observed in SW480/shDDX39B group (Fig. 3B). Additionally, qRT-PCR was used to detect the mRNA expression level of MMP3/7/9/14, the results of which were similar (Fig. S3A). Furthermore, F-actin staining was conducted to evaluate the transformation of the cytoskeleton. SW480/DDX39B cells exhibited a spindle-like, fibroblastic morphology and the rearrangement of F-actin fibers, while cells in SW480/shDDX39B group showed a round or flat morphology (Fig. 3C).

Consistent with these findings, IHC and immunofluorescence analysis of orthotopic cecal tumors from the mice showed the increased expression of Vimentin and MMP9 and decreased expression of E-cadherin in SW480/Scramble group compared to SW480/shDDX39B group (Fig. 3D).

DDX39B modulates FUT3 expression by regulating mRNA splicing and export

Gene set enrichment analysis (GSEA) showed that DDX39B is closely related to mRNA binding, RNA splicing and nuclear export (Fig. 4A-C). Similar results were found in an enrichment analysis of GO- Cellular components (Fig. S3C).^[26] The RNA-seq results revealed altered gene expression levels in SW480/DDX39B group (Supplementary sheet 2). qRT-PCR assay was conducted to validate changes in mRNA levels. As shown in Figure 4D, the mRNA expression level of FUT3 was significantly altered by DDX39B upregulation.

Thus, we explored the function of FUT3 in CRC cells. As shown in Figure S2A, FUT3 was highly expressed in CRC (TCGA database online website GEPIA^[27]). Additionally, overall survival analysis showed that CRC patients with high level of FUT3 had a shorter overall survival time (Fig. S2B), result from PROGeneV2-Pan Cancer Prognostic Database was in line with the finding (Fig. S2C). Moreover, Transwell and wound healing assay presented that FUT3 could promoted the migration and invasion ability of CRC cells (Fig. S2D). Western blotting showed that silenced FUT3 might down-regulate the EMT markers, SMADs and MMPs (Fig. S2E).

Furthermore, we explored the correlation between DDX39B and FUT3. IHC staining of serial CRC tissues sections (3/10 paired) exhibited that the change in DDX39B expression may be correlated with the altered FUT3 expression (Fig. 4H). In addition, DDX39B mRNA expression level was found to be positively correlated with the FUT3 mRNA expression level in both paired CRC tissues and cell lines (Fig. 4F-G). Next, we explored the localization of FUT3 using a nuclear and cytoplasmic separation assay. The expression of FUT3 was altered mainly in the cytoplasm, while the expression of DDX39B was mainly in the nucleus (Fig. 5B). Similar results were obtained with the immunofluorescence assay (Fig. S2F).

To further investigate the direct role of DDX39B in regulating the expression of FUT3, we analyzed the mutual effects of DDX39B and FUT3 using a networks dataset from the STRING database, which showed that DDX39B, tether with ALYREF, may recruit a complex such as EJC (MAGOH/MAGOHB/EIF4A3) or TREX (THOC1-3) to affect FUT3 (Fig. 4I). Next, we carried out RIP, the result of which showed that DDX39B binds the first exon of FUT3, and confirmed the binding sequence by DNA sequencing (Fig. 4J-S3B). Nuclear and cytoplasmic RNA separation assay demonstrated that the fold change in FUT3 expression was higher in the cytoplasm than in the nucleus (Fig. 4K), suggesting that DDX39B enhances mRNA export of FUT3. Furthermore, there are four transcripts whose products could be translated to FUT3 protein with fully function. At the splicing level, qRT-PCR using primers in exon 1 (all transcripts own) and complete exon 2 (only transcript NM_000149.3 owns) revealed that there is more variation of FUT3 mRNA level in products contain longer exon 2. Therefore, DDX39B may favor the inclusion of longer FUT3 exon 2 (Figure 4L). Together with the RNA-seq results which only detected the increased FUT3 transcript NM_000149.3 (not shown), suggesting that DDX39B may regulates the alternative splicing of FUT3.

DDX39B enhanced the invasive prosperity of CRC cells via TGFβ signaling pathway through L-fucosylated TGFβR-I by FUT3

Lectin blotting analysis showed decreased L-fucosylated TGFβR-I in SW480 cells with DDX39B knockdown and increased L-fucosylated TGFβR-I in SW480 cells with DDX39B overexpression (Fig. 5A). Costaining for TGFβR-I and AAL presented that TGFβR-I levels remained constant in SW480 cells upon DDX39B overexpression or silencing, while AAL levels were altered.

Therefore, we analyzed the changes in the expression of certain important genes in the TGFβ signaling pathway. Assays of nuclear and cytoplasmic protein separation showed that DDX39B silencing inhibits SMAD2 and SMAD3 phosphorylation and nuclear localization, while overexpressed DDX39B had the opposite effect (Fig. 5B). Furthermore, SW480/DDX39B cells was treated in an inhibitor of TGFβ signaling pathway (SB431542), western blotting and

Transwell assay showed that SB431542 abrogated the effect of DDX39B in enhancing the TGF β signaling pathway and reduced the effect of DDX39B in facilitating CRC metastasis (Fig. 5C-D).

Next, we assessed whether cells in the SW480/shDDX39B group were responsive to TGF β 1. TGF β 1 did not induce the expression of downstream SAMDs and EMT markers in SW480/shDDX39B group but triggered the expression of SMADs and EMT markers in SW480/Scramble group (Fig. 6A). SW480/Scramble cells exhibited increased migration and invasion after TGF β 1 treatment than SW480/shDDX39B cells (Fig. 6B, Fig. S3D). Consistent with these findings, immunofluorescence to detect E-Cadherin and Vimentin also demonstrated that TGF β 1 did not elicit the expression of EMT markers in SW480/shDDX39B cells but did induce the expression of these proteins in SW480/Scramble cells (Fig. 6E).

Then, we analyzed the capacity of FUT3 to enhance DDX39B-mediated activation of the TGF β /SMAD2 signaling pathway. Western blotting and Transwell assays revealed that the suppression of FUT3 by siRNA could partly alleviate the effect of DDX39B upregulation on TGF β /SMAD2 pathway activation (Fig. 6C-D, Fig. S3E).

Discussion

The DDX family is implicated in many steps of RNA metabolism, and the exact function of each DDX is determined by its environment or binding partners. DDX39B is localized in nuclear speckles where most mRNA transcription and splicing occur^[28], so its core obligation is mRNA splicing and export, which may influence later steps of gene expression. Therefore, deregulation of DDX39B may exert deleterious effects on mRNA splicing/export, thus influencing the expression and function of key proteins. Though the functions of DDXs in cancers have recently been highly examined, the exact contribution of DDX39B in CRC has not yet been investigated. Our data suggested that DDX39B overexpression in CRC promoted the aggravation of CRC, which indicated that DDX39B may serve as a tumor promoter in the development of CRC and thus needs to be thoroughly characterized.

Therefore, we sought to determine how abnormal expression of DDX39B disrupts cellular function and enhances CRC thrive. Considering that protein-protein interactions are essential for RNA helicases to carry out their functions, we assumed that DDX39B exerts effects on the downstream by forming certain complex. DDX39B was reported to be bound to mRNA during splicing, and DDX39B is retained on spliced mRNA in the exon as part of the EJC or TREX^[28]. Specifically, RNA nuclear export is splicing-dependent and is coupled to RNA splicing, and in one model, once DDX39B, a splice factor, helps U2 snRNP attach to the splicing branch point, DDX39B could tether with ALYREF and other components to recruit the EJC or TREX for mRNA export.^[29] In our study, RIP showed that DDX39B binds the first exon of FUT3 mRNA, near the splice branch point and upstream of the EJC binding site. STRING analysis revealed that the effect of DDX39B on FUT3 may occur through its association with ALYREF, which recruits the EJC (MAGOH/MAGOHB) or TREX(THOC1-3). Additionally, the results of cytoplasmic and nuclear RNA separation revealed that the fold change in FUT3 mRNA levels in the cytoplasm was higher than in the nucleus, suggesting enhanced mRNA export. So we assumed that DDX39B affects FUT3 mRNA splicing and export. Moreover, RNA-seq results and qRT-PCR showed that overexpressed DDX39B favor the longer FUT3 mRNA products that contain the complete and longer exon 2, suggesting an alternative splicing of FUT3. Recognition of the regulatory role of DDX39B in RNA metabolism is an important step in increasing our understanding of FUT3 mRNA splicing and export evoked by DDX39B, a key component of the spliceosome and mRNA transcription export complex. Further study is required to clarify how DDX39B participates in the alternatives splicing and export of FUT3 mRNA.

Protein glycosylation is an important type of posttranslational modification. Much data has revealed that abnormal glycosylation due to the aberrant expression of glycosylation transferases is closely correlated with tumor progression and metastasis.^[30-32] FUT3, a kind of fucosyltransferases, adds L-fucose in an $\alpha(1,4)$ linkage to GlcNAc residues in sialylated precursors to synthesize CA199.^[33,34] A previous study demonstrated that abnormal expression of FUT3 contributes to aberrant fucosylation of TGF β R-I, eventually causing abnormal activation of the TGF β signaling pathway.^[35] Our study demonstrated that FUT3 is overexpressed in CRC and regulated by DDX39B. Additionally, our results showed inefficient fucosylation of TGF β R-I with DDX39B knockdown, and overexpression had the opposite effects. Aberrant fucosylation of TGF β Rs induced by FUT6/FUT8 has also been observed in some studies.^[35,36] Our data (RNA-seq) showed that DDX39B does not modulate the expression of fucosyltransferases (FUTs) other than FUT3.

The TGF β signaling pathway is an important cellular pathway that regulates many processes and plays a significant role in cellular proliferation, differentiation and apoptosis. TGF β R-I, an essential part of the canonical TGF β signaling pathway, the alteration of it could affect the activation of the TGF β signaling pathway. In our case, DDX39B intervened in the TGF β /Smad2 signaling pathway by upregulating FUT3 and catalyzing the fucosylation of TGF β R-I, after which the activated TGF β /Smad signaling pathway upregulated expression of MMPs and the EMT transcriptional factors like Snail, Slug, ZEB1. MMPs can degrade basement membrane components to promote tumor cell infiltration in the blood systems. Together with EMT, a decrease in epithelial markers (E-cadherin) and increase in mesenchymal markers (Vimentin) drive the reduced adhesion of cells and loss of cell polarity and eventually contribute to CRC progression.

Conclusions

In conclusion, DDX39B acts as a tumor promoter in CRC through upregulating the expression of FUT3 and then promoting the fucosylation of TGF β R-I, subsequently enhancing activation of the TGF β /SMAD signaling pathway to facilitate the invasion and metastasis of CRC. Taken together, the findings on the DDX39B/FUT3/TGF β R-I axis might provide new insight into the CRC tumorigenesis and suggest that the proteins in this axis can be applied as molecular markers for CRC detection or treatment.

List Of Abbreviations

COAD: Colon adenocarcinoma; DDX: DEAD box; CRC: Colorectal cancer; EMT: Epithelial-mesenchymal transition. ECM: Extracellular matrix; EJC: Exon-junction complex; TREX: Transcription-export complex. RNA-seq: RNA sequencing; RIP: RNA binding protein immunoprecipitation; qRT-PCR : Quantitative real-time PCR.

Declarations

Ethics approval and consent to participate

All patients were informed of sample usage and collection. And the protocols used in this study were approved by NanFang Hospital's Protection of Human Subjects Committee. The animal protocols were approved by the Use Committee for Animal Care.

Consent for publication

All the authors listed have approved the manuscript enclosed and consent for publication.

Availability of data and materials

All data analyzed during this study are included in this manuscript.

Competing interests

The authors declare that they have no competing financial or other interests to disclose.

Funding

This study was supported by Guangdong Science and Technology Project (No.2017B020209003), Guangdong Medical Science and Technology Research Fund (No.A2020143), and the Foundation for the President of Nanfang Hospital.

Author's contributions

CCH and AML performed the experiments and wrote the manuscript. QHL, JD and QY helped to analyzed and performed the experiments. SDL and QYL designed and supervised the study. All authors have read and proved the final manuscript.

Acknowledgements

Not applicable.

References

1. Siegel RL, Miller KD. Colorectal cancer statistics, 2020. *CA Cancer J Clin.* 2020;70(3):145-164.
2. Leivonen SK, Kähäri VM. Transforming growth factor-beta signaling in cancer invasion and metastasis. *Int. J. Cancer.* 2007;121(10):2119-2124.
3. Hao Y, Baker D, Ten Dijke P. TGF- β -Mediated Epithelial-Mesenchymal Transition and Cancer Metastasis. *Int. J. Mol. Sci.* 2019;20(11):2767.
4. Batlle R, Andrés E, Gonzalez L, et al. Regulation of tumor angiogenesis and mesenchymal-endothelial transition by p38 α through TGF- β and JNK signaling. *Nat. Commun.* 2019;10(1):3071.
5. Li F, Shi J, Xu Z, et al. S100A4-MYH9 Axis Promote Migration and Invasion of Gastric Cancer Cells by Inducing TGF- β -Mediated Epithelial-Mesenchymal Transition. *J. Cancer.* 2018;9(21):3839-3849.
6. Xu F, Zhang J, Hu G, et al. Hypoxia and TGF- β 1 induced PLOD2 expression improve the migration and invasion of cervical cancer cells by promoting epithelial-to-mesenchymal transition (EMT) and focal adhesion formation. *Cancer Cell Int.* 2017;17:54.
7. Wang X, Lai Q, He J, et al. LncRNA SNHG6 promotes proliferation, invasion and migration in colorectal cancer cells by activating TGF- β /Smad signaling pathway via targeting UPF1 and inducing EMT via regulation of ZEB1. *Int J Med Sci.* 2019;16(1):51-59.
8. Linder P, Jankowsky E. From unwinding to clamping - the DEAD box RNA helicase family. *Nature reviews. Mol Cell Biol.* 2011;12(8):505-516.
9. Silverman E, Edwalds-Gilbert G, Lin RJ. DEXD/H-box proteins and their partners: helping RNA helicases unwind. *Gene.* 2003;312:1-16.
10. Kouyama Y, Masuda T, Fujii A, et al. Oncogenic splicing abnormalities induced by DEAD-Box Helicase 56 amplification in colorectal cancer. *Cancer Sci.* 2019;110(10):3132-3144.
11. Germann S, Gratadou L, Zonta E, et al. Dual role of the ddx5/ddx17 RNA helicases in the control of the pro-migratory NFAT5 transcription factor. *Oncogene.* 2012;31(42):4536-4549.
12. Tang J, Chen H, Wong CC, et al. DEAD-box helicase 27 promotes colorectal cancer growth and metastasis and predicts poor survival in CRC patients. *Oncogene.* 2018;37(22):3006-3021.
13. Taniguchi I, Ohno M. ATP-dependent recruitment of export factor Aly/REF onto intronless mRNAs by RNA helicase UAP56. *Mol Cell Biol.* 2008;28(2):601-608.
14. Shen H. UAP56- a key player with surprisingly diverse roles in pre-mRNA splicing and nuclear export. *BMB Rep.* 2009;42(4):185-188.
15. Fleckner J, Zhang M, Valcárcel J, et al. U2AF65 recruits a novel human DEAD box protein required for the U2 snRNP-branchpoint interaction. *Genes Dev.* 1997;11(14):1864-1872.

16. Shen H, Zheng X, Shen J, et al. Distinct activities of the DExD/H-box splicing factor hUAP56 facilitate stepwise assembly of the spliceosome. *Genes Dev.* 2008;22(13):1796-1803.
17. Luo ML, Zhou Z, Magni K, et al. Pre-mRNA splicing and mRNA export linked by direct interactions between UAP56 and Aly. *Nature.* 2001;413(6856):644-647.
18. Kuramitsu Y, Tominaga W, Baron B, et al. Up-regulation of DDX39 in human malignant pleural mesothelioma cell lines compared to normal pleural mesothelial cells. *Anticancer Res.* 2013;33(6):2557-60.
19. Kuramitsu Y, Suenaga S, Wang Y, et al. Up-regulation of DDX39 in human pancreatic cancer cells with acquired gemcitabine resistance compared to gemcitabine-sensitive parental cells. *Anticancer Res.* 2013;33(8):3133-6.
20. Kato M, Wei M, Yamano S, et al. DDX39 acts as a suppressor of invasion for bladder cancer. *Cancer Sci.* 2012;103(7):1363-1369.
21. Sugiura T, Nagano Y, Noguchi Y. DDX39, upregulated in lung squamous cell cancer, displays RNA helicase activities and promotes cancer cell growth. *Cancer Biol Ther.* 2007;6(6):957-964.
22. Zhang T, Ma Z, Liu L, et al. DDX39 promotes hepatocellular carcinoma growth and metastasis through activating Wnt/ β -catenin pathway. *Cell Death Dis.* 2018;9(6):675.
23. Chandrashekar DS, Bashel B, Balasubramanya SAH, et al. UALCAN: A Portal for Facilitating Tumor Subgroup Gene Expression and Survival Analyses. *Neoplasia (New York, N.Y.).* 2017;19(8):649-658.
24. Li Q, Lai Q, He C, et al. RUNX1 promotes tumour metastasis by activating the Wnt/ β -catenin signalling pathway and EMT in colorectal cancer. *J Exp Clin Cancer Res.* 2019;38(1):334.
25. Pino MS, Kikuchi H, Zeng M, et al. Epithelial to mesenchymal transition is impaired in colon cancer cells with microsatellite instability. *Gastroenterology.* 2010;138(4):1406-1417.
26. Liao Y, Wang J, Jaehnig EJ, et al. WebGestalt 2019: gene set analysis toolkit with revamped UIs and APIs. *Nucleic Acids Res.* 2019;47(W1):W199-w205.
27. Tang Z, Li C, Kang B, et al. GEPIA: a web server for cancer and normal gene expression profiling and interactive analyses. *Nucleic Acids Res.* 2017;45(W1):W98-w102.
28. Kota KP, Wagner SR, Huerta E, et al. Binding of ATP to UAP56 is necessary for mRNA export. *J Cell Sci.* 2008;121(Pt 9):1526-1537.
29. Cheng H, Dufu K, Lee CS, et al. Human mRNA export machinery recruited to the 5' end of mRNA. *Cell.* 2006;127(7):1389-1400.
30. Glavey SV, Huynh D, Reagan MR, et al. The cancer glycome: carbohydrates as mediators of metastasis. *Blood Rev.* 2015;29(4):269-279.
31. Magalhães A, Duarte HO, Reis CA. Aberrant Glycosylation in Cancer: A Novel Molecular Mechanism Controlling Metastasis. *Cancer cell.* 2017;31(6):733-735.
32. Josic D, Martinovic T, Pavelic K. Glycosylation and metastases. *Electrophoresis.* 2019;40(1):140-150.
33. Miyazaki K, Ohmori K, Izawa M, et al. Loss of disialyl Lewis(a), the ligand for lymphocyte inhibitory receptor sialic acid-binding immunoglobulin-like lectin-7 (Siglec-7) associated with increased sialyl Lewis(a) expression on human colon cancers. *Cancer Res.* 2004;64(13):4498-505.
34. Tsuchida A, Okajima T, Furukawa K, et al. Synthesis of disialyl Lewis a (Le(a)) structure in colon cancer cell lines by a sialyltransferase, ST6GalNAc VI, responsible for the synthesis of alpha-series gangliosides. *J Biol Chem.* 2003;278(25):22787-22794.
35. Hirakawa M, Takimoto R, Tamura F, et al. Fucosylated TGF- β receptors transduces a signal for epithelial-mesenchymal transition in colorectal cancer cells. *Brit J Cancer.* 2014;110(1):156-163.
36. Lin H, Wang D, Wu T, et al. Blocking core fucosylation of TGF- β 1 receptors downregulates their functions and attenuates the epithelial-mesenchymal transition of renal tubular cells. *Am J Physiol Renal Physiol.* 2011;300(4):F1017-1025.

Figures

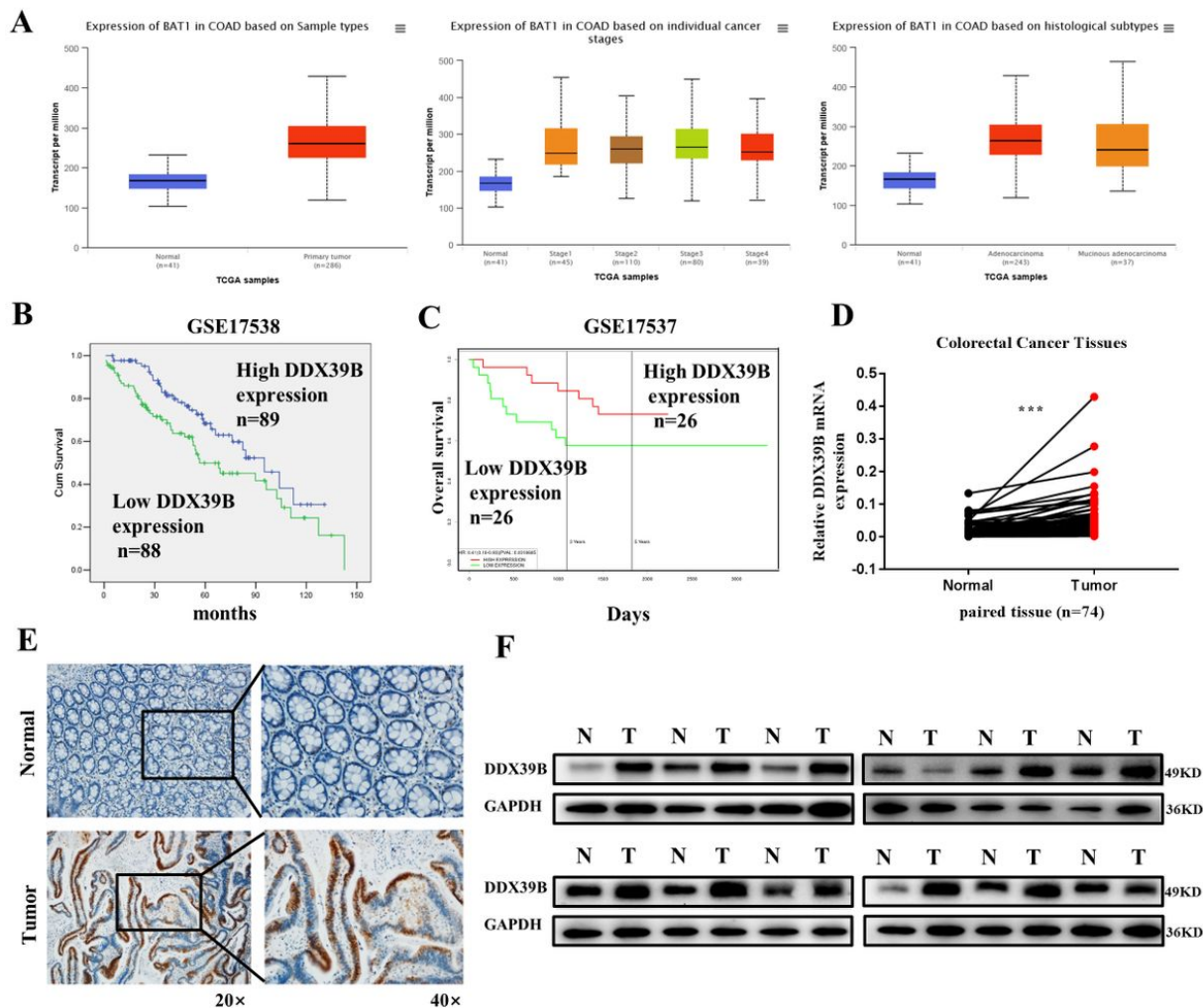


Figure 1

DDX39B expression in colorectal cancer tissues. A. DDX39B/BAT1 was overexpressed in CRC samples and the expression of DDX39B varies in different histological types and cancer stages (TCGA Dataset). B. Overall survival with low/high DDX39B expression was obtained from a colorectal cancer set of GSE17538. C. Overall survival with low/high DDX39B expression was analyzed using GSE17537. D. DDX39B mRNA expression detected by qPCR in colorectal cancer tissues and paired non-cancerous tissues (n=74). E. IHC analysis of 20 pairs colorectal cancer and adjacent non-tumor tissues. F. Expression of DDX39B protein was detected in 12 pairs of colorectal cancer tissues and paired normal tissues.

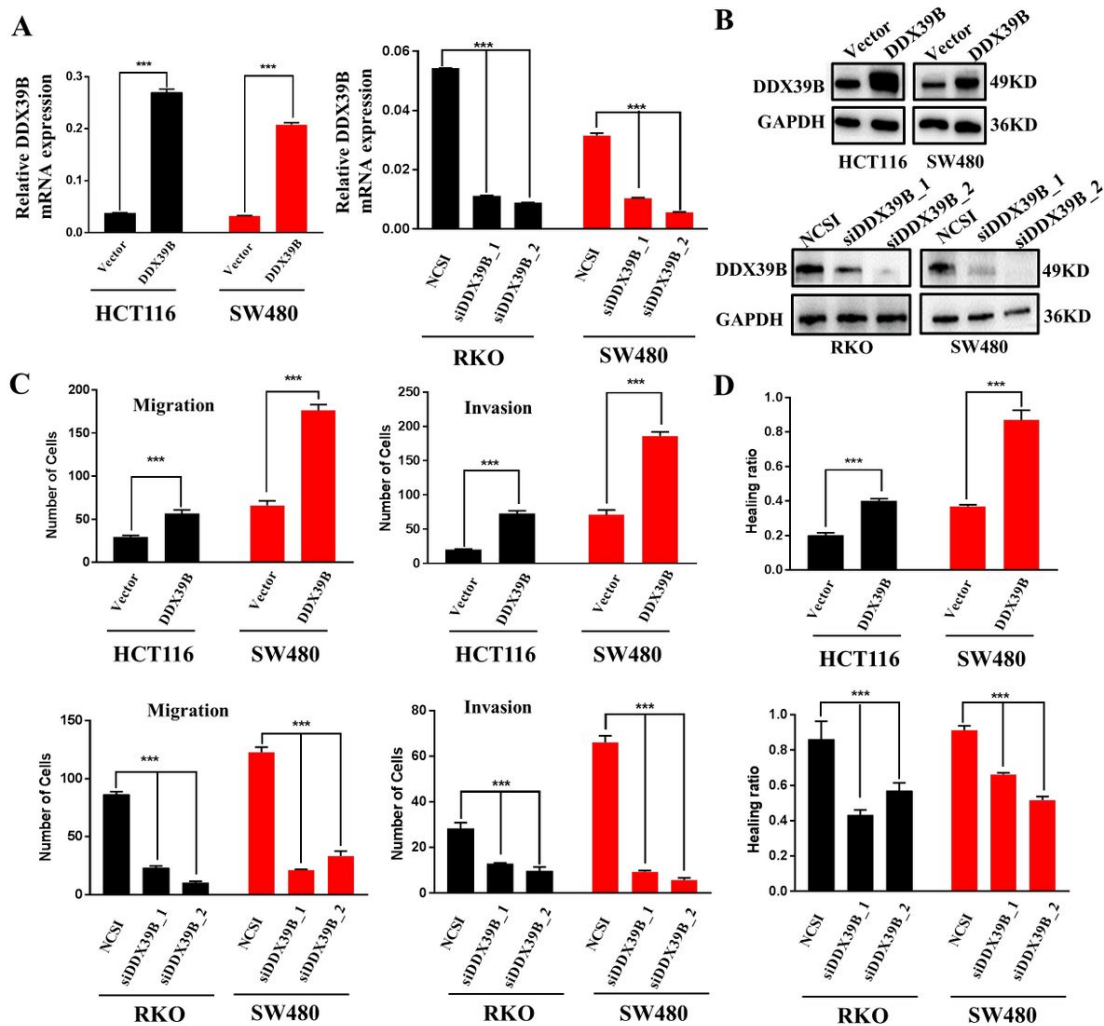


Figure 2

DDX39B enhanced the migration and invasion ability of CRC in vitro. A-B. Transfected efficiency were determined by western blotting and qPCR in HCT116, SW480 and RKO cells with DDX39B overexpressed and silenced. C. Migration and invasion abilities were evaluated by Transwell assay in HCT116, SW480 and RKO cells with DDX39B overexpressed and silenced. D. Migration capacity was assessed by Wound healing assay in HCT116, SW480 and RKO cells with DDX39B overexpressed and silenced.

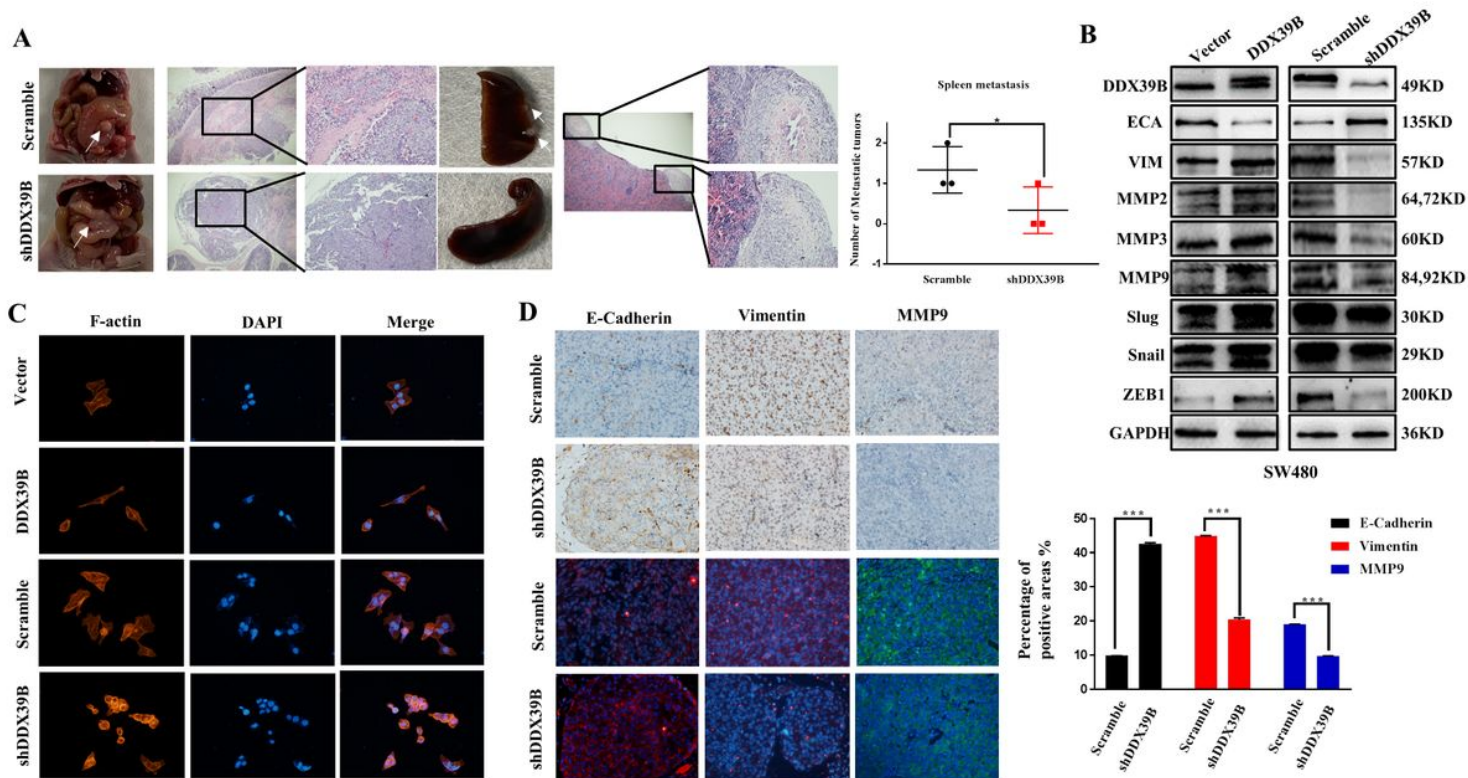


Figure 3

DDX39B promotes CRC metastasis in vitro and EMT. A. HE staining of Orthotopic transplantation tumor of CRC and spleen metastasis in SW480/Scramble and SW480/shDDX39B group. Spleen metastases were also compared between these groups. B. Expression of EMT markers and MMPs were evaluated in SW480 cells with DDX39B overexpressed and knockdown. C. Cytoskeleton assessed by FITC-phalloidine staining in SW480 cells with DDX39B overexpressed and knockdown. D. IHC and immunofluorescence of Orthotopic transplantation tumor in mice were conducted. Expression of E-cadherin, Vimentin and MMP9 were compared in SW480/Scramble and SW480/shDDX39B group. Relevant pathological scores of each were also obtained.

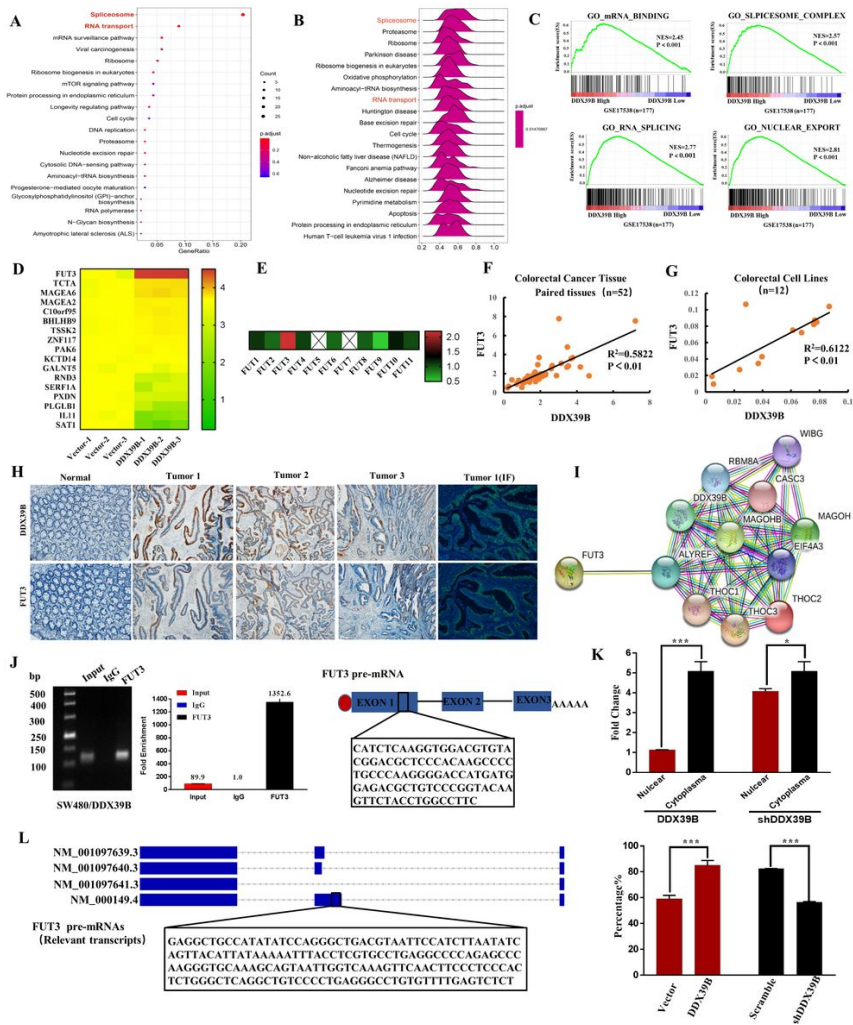


Figure 4

DDX39B modulates FUT3 expression via regulating mRNA splicing and export. A-B. Enrichment analysis using KEGG and GSEA showed RNA export and splice were enriched in CRC with DDX39B expression. C. Relationship of certain RNA processes with low/high DDX39B expression were shown using GSE17538 (n=177). D. qRT-PCR assay was conducted to validate the fold changes in certain gene expression (RNA-seq results) in SW480/Vector and SW480/DDX39B group. E. Fold changes of FUT family members were assessed by qPCR in SW480/Vector and SW480/DDX39B group (RNA-seq results). F. Correlation between DDX39B and FUT3 expression was assessed by qPCR in 52 paired CRC tissues. G. Correlation between DDX39B and FUT3 expression was evaluated by qPCR in 12 CRC/normal colon cells. H. IHC of serial paired CRC tissues (3/10) were performed to analyze the correlation between FUT3 and DDX39B expression. I. DDX39B interacting with FUT3 as a part of EJC/TREX was shown using STRING. J. RIP assay in SW480/DDX39B cells showed DDX39B binds the first exon of FUT3 mRNA. K. Nuclear and cytoplasmic separation assay was conducted to assess the fold change of FUT3 mRNA expression in SW480 cells with DDX39B overexpressed and silenced. L. The expression level of FUT3 splicing variants (corresponding to different transcripts), detected by qRT-PCR using different primers.

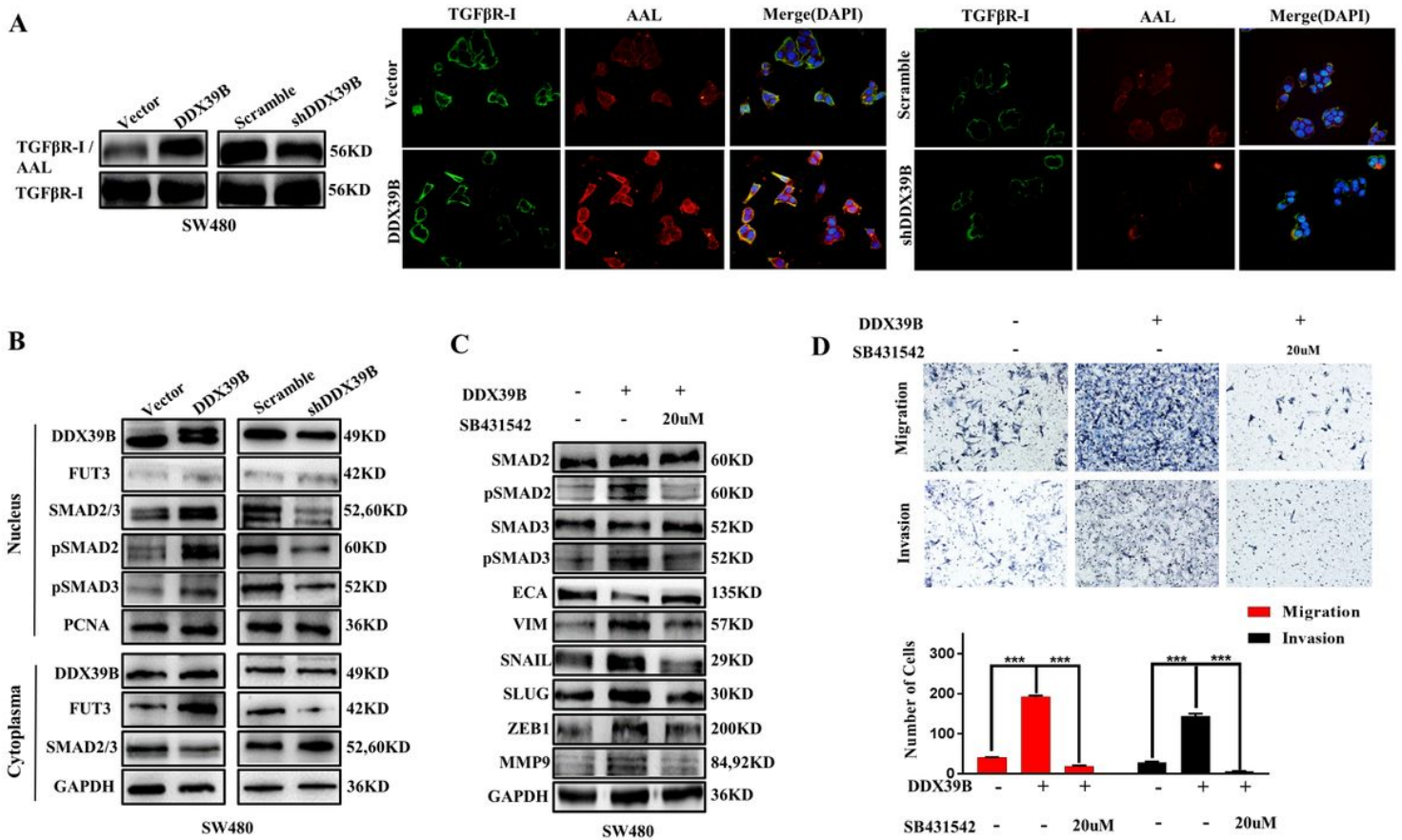


Figure 5
 DDX39B enhances the invasive prosperities of colorectal cancer cell via TGF β signaling pathway through L-fucosylated TGF β R I by FUT3. A. immunofluorescence and lectin blotting to detect AAL and TGF β R-I were analyzed in SW480 cells with DDX39B overexpressed and silencing. B. Nuclear and cytoplasmic separation assay was conducted to assess FUT3 and targeted gene expression of TGF β signaling pathway in SW480 cells with DDX39B overexpressed and silencing. C. Expressions of EMT markers and targeted gene expression of TGF β signaling pathway were detected by western blotting in SW480/Vector and SW480/DDX39B cells with SB431542(0/20 μ M) treated. D. Migration and invasion abilities were assessed by Transwell assay in SW480/Vector and SW480/DDX39B cells with SB431542(0/20uM) treated.

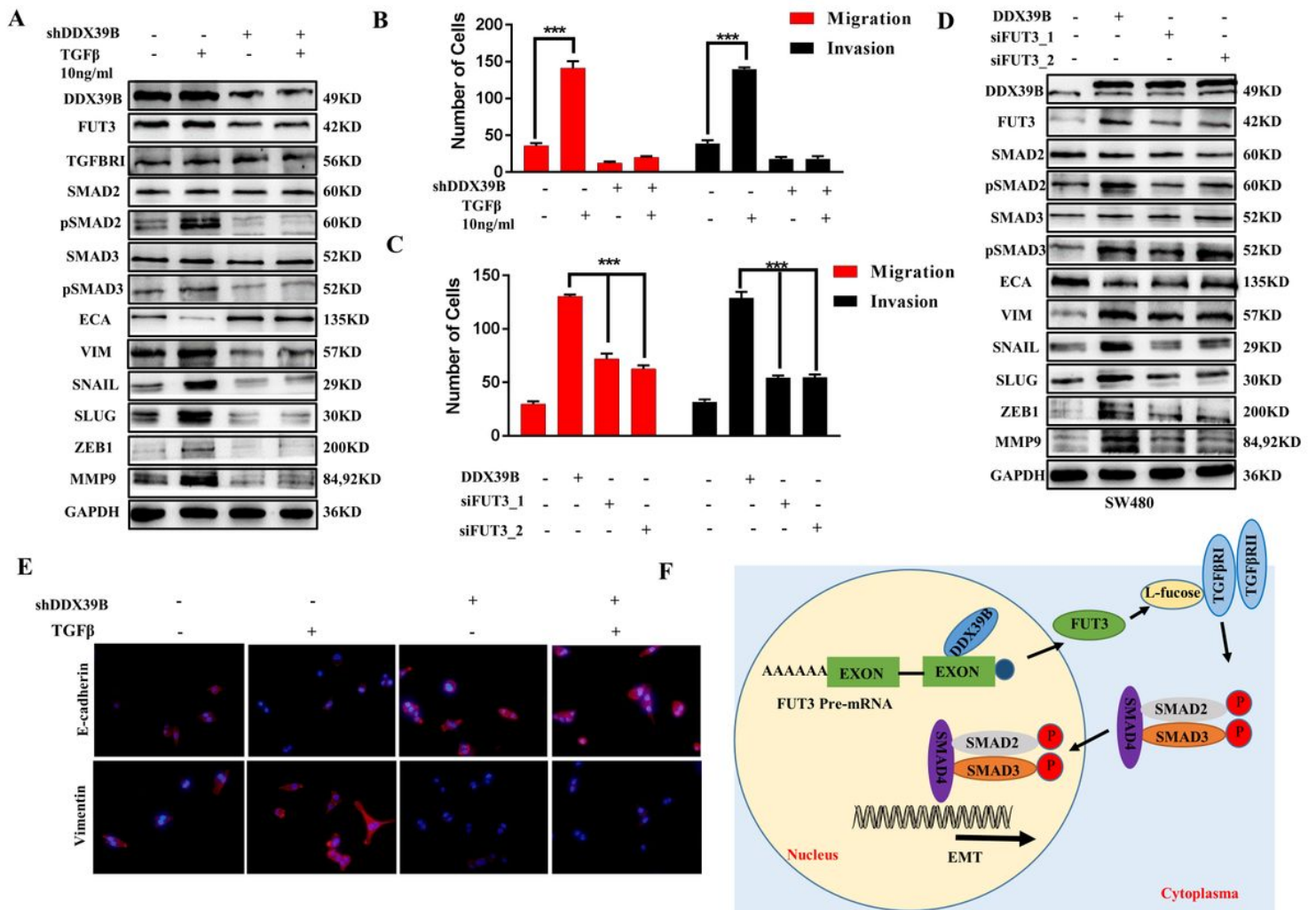


Figure 6

The DDX39B-FUT3-TGFβRI axis promotes CRC metastasis and EMT. A. Expression of FUT3 and targeted gene of TGFβ signaling pathway and EMT markers were detected by western blotting in SW480/Scramble and SW480/shDDX39B cells with TGFβ treated. B. Migration and invasion abilities were assessed by Transwell assay in SW480/Scramble and SW480/shDDX39B cells with TGFβ treated (10ng/ml). C. Migration and invasion abilities were assessed by Transwell assay in SW480/Vector and SW480/DDX39B cells with FUT3 knockdown. D. Expression of FUT3, targeted gene of TGFβ signaling pathway and EMT were detected by western blotting in SW480/Vector and SW480/DDX39B cells with FUT3 silenced. E. Immunofluorescence to detect E-cadherin and Vimentin in SW480/Scramble and SW480/shDDX39B cells with TGFβ treated. F. Hypothesized molecular mechanism of DDX39B in the development of CRC.

Supplementary Files

This is a list of supplementary files associated with this preprint. Click to download.

- [Supplementaryfile.docx](#)
- [Supplementaryfile.docx](#)
- [Supplementarysheet1RNAseqresults.xlsx](#)
- [Supplementarysheet1RNAseqresults.xlsx](#)
- [TableS3SequencesofsiRNAs.docx](#)
- [TableS3SequencesofsiRNAs.docx](#)
- [TableS2PrimersequencesusedforqRTPCR.docx](#)
- [TableS2PrimersequencesusedforqRTPCR.docx](#)
- [TableS1SupplementaryMaterialsandMethods.docx](#)
- [TableS1SupplementaryMaterialsandMethods.docx](#)
- [SupplementaryFigure3.tif](#)
- [SupplementaryFigure3.tif](#)

- SupplementaryFigure2.tif
- SupplementaryFigure2.tif
- SupplementaryFigure1.tif
- SupplementaryFigure1.tif